Aerospace Science and Technology 32 (2014) 162–168

Contents lists available at ScienceDirect

Aerospace Science and Technology

www.elsevier.com/locate/aescte

Low-Reynolds-number effect on the aerodynamic characteristics of a pitching NACA0012 airfoil

Dong-Ha Kim [a,1], Jo-Won Chang [b,*,2]

[a] Korean Air R&D Center, Daejeon Metropolitan City, 305-811, Republic of Korea
[b] Korea Aerospace University, Goyang City, Gyeonggi-do, 412-791, Republic of Korea

ARTICLE INFO

Article history:
Received 24 December 2012
Received in revised form 27 August 2013
Accepted 29 August 2013
Available online 10 September 2013

Keywords:
Low-Reynolds-number effect
Unsteady aerodynamic characteristics
Pitching airfoil
NACA0012

ABSTRACT

The effect of a low Reynolds number in the range of $2.0 \times 10^4 < Re_c < 5.0 \times 10^4$ on the aerodynamic characteristics of a pitching NACA0012 airfoil was investigated. Reverse flow and near wake were visualized by smoke-wire flow visualization, and lift and pressure drag coefficients were estimated by measuring unsteady pressure through pressure distortion correction. A NACA0012 airfoil sinusoid-pitched at quarter chord was employed, and its mean angle of attack and oscillation amplitude were $\alpha = 0°$ and 6° respectively. The test Reynolds numbers were $Re_c = 2.3 \times 10^4$, 3.3×10^4 and 4.8×10^4 with a fixed reduced frequency of $K = 0.1$. Through reverse flow visualization, the first and second trailing-edge vortices and mushroom structure depending on the Reynolds number were observed. In lift and pressure drag coefficients, hysteresis loops were comparatively varied with the Reynolds number. As a result, the phase angle, at which boundary-layer events occurred, was in inverse proportion to the increase in Reynolds number. This result implies that the increase in Reynolds number promotes the occurrence of boundary-layer events such as laminar separation and transition.

1. Introduction

Recent advances in the performance of MAVs have led to increasing research interest in these vehicles, and the development of such airplanes has focused on *biomimetics*. Most MAVs are operated under the condition of unsteady flow with moving wings, and their operational Reynolds number range is very low due to their small size and low free-stream velocity [7]. In a low-Reynolds-number range, the boundary-layer characteristics on a static airfoil surface can be divided into four regimes, laminar, subcritical, transitional, and supercritical, which are dependent on the Reynolds number and the angle of attack [8]. This detail implies that boundary-layer events are dramatically sensitive to Reynolds number. Kim et al. [12], Laitone [15,16], and Feng et al. [6] investigated the aerodynamic characteristics in a low-Reynolds-number range of a static airfoil, a static wing (aspect ratio 6), and a gurney flap with plasma actuator, respectively. In their results, lift and drag coefficients were nonlinearly varied due to the low-Reynolds-number effect. These results are clearly different from the classical results.

For a pitching airfoil, which is regarded as a representative example of an unsteady flow, the most important ingredients are oscillating amplitude, mean angle of attack, reduced frequency [2], and Reynolds number. Dynamic stall is commonly studied by researchers because wing motion amplitude is very large above the stall angle. Beyond the stall angle, oscillating amplitude and mean angle of attack are the dominant parameters [19,20] because they affect leading-edge vortex (LEV) and trailing-edge vortex (TEV) formations, which determine aerodynamic performance in dynamic stall. Meanwhile, acceleration effect critically influences boundary-layer events within the stall angle [4,5], and it is dominantly dependent on pitching direction. Kim et al. [13] measured the unsteady pressure coefficient through the pressure distortion correction that occurred for a pitching airfoil at $Re_c = 4.8 \times 10^4$ within stall angle ($\alpha_a = \pm 6°$). In their study, the unsteady pressure coefficient on the airfoil surface dramatically varied with pitching direction.

For an unsteady flow in a low-Reynolds-number range, boundary-layer events are very complicated and ambiguous. For a pitching airfoil, the separation point does not correspond to zero shear stress [22,24], and the disappearance of shear stress and reverse flow is no longer an indicator of the separation for the oscillating boundary layer [3,14]. Kim and Chang [10] investigated an unsteady boundary layer for a pitching airfoil and suggested an unsteady laminar separation mechanism that has a different definition from laminar separation. The unsteady laminar separation occurred after the reattachment of the separated shear layer, and the inflection point inside the unsteady boundary layer was suggested at the point comprising two counter-rotating vortices, a wall and

* Corresponding author.
E-mail address: jwchang@kau.ac.kr (J.-W. Chang).
[1] Researcher, Aerodynamics Group.
[2] Professor, Department of Aeronautical Science and Flight Operation.

1270-9638/$ – see front matter
http://dx.doi.org/10.1016/j.ast.2013.08.018

Nomenclature

C	airfoil chord length	U_∞	free-stream velocity
C_l	lift coefficient	α	angle of attack
C_d	pressure drag coefficient	α_a	oscillating amplitude
C_p	pressure coefficient	$\alpha_{unsteady}$	maximum angle of attack for a pitching airfoil
f	oscillating frequency (Hz)	α_{static}	angle of attack for a static airfoil
K	reduced frequency $K = \pi fC/U_\infty$	α_u	angle of attack during upstroke motion
Re_c	Reynolds number based on airfoil chord length	α_d	angle of attack during downstroke motion
t	time	ω	angular velocity

external flow. These flow structures are predominantly influenced by the Reynolds number and therefore, the unsteady boundary layer in low-Reynolds-number range should be elaborately investigated for their application to various flow fields.

The objective of this paper is to investigate the low-Reynolds-number effect on the aerodynamic characteristics of a pitching airfoil within a stall angle. Kim and Chang [10] qualitatively depicted a flow structure inside an unsteady boundary layer using smoke-wire visualization. Kim et al. [12] described the low-Reynolds-number effect for a static airfoil. Kim et al. [13] also discussed the unsteady pressure characteristics of a pitching airfoil at a low Reynolds number. In contrast to previous studies [10,12,13], the present paper quantitatively elucidates the unsteady aerodynamic characteristics with respect to chronologically changed Reynolds number. As mentioned earlier, boundary-layer events are abruptly varied with a Reynolds number in a low range and, its lift and drag coefficients will be dramatically varied according to the variation of the small Reynolds number. This is the main research motivation of the current study. Here, Reynolds number varies in the range of $2.0 \times 10^4 < Re_c < 5.0 \times 10^4$ with the fixed reduced frequency of $K = 0.1$, and unsteady pressure is measured through pressure distortion correction that occurs in pneumatic tubing [9,13,23]. A pressure transducer that can measure low pressure with high accuracy is employed. To obtain physical insight into the flow structure, reverse flow and near wake are visualized by smoke-wire flow visualization. In Section 3, flow visualization, unsteady pressure distribution and aerodynamic characteristics are discussed.

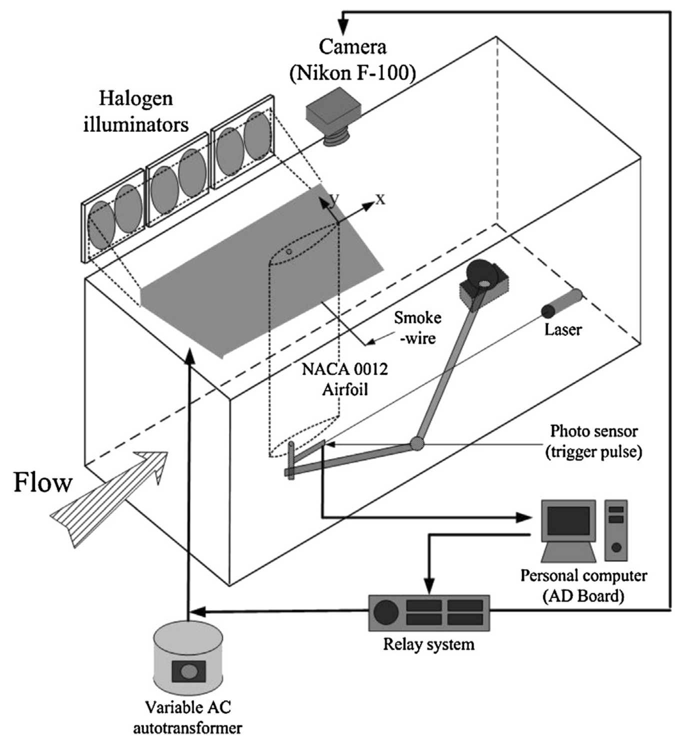

Fig. 1. Schematic of test section and flow visualization system.

2. Experimental setup and procedure

Fig. 1 shows the schematic of the test section and reverse flow visualization system. Experiments were conducted in a low-speed wind tunnel, which is an open suction type tunnel with a test-section size of 0.5 m (H) × 0.5 m (W) × 1.4 m (L). The cross section of the airfoil model was a NACA0012 with a chord length of 0.18 m. The airfoil was vertically installed in the test section. To minimize the three-dimensional effect, the gap between the test-section side wall and the airfoil was set to less than 2.5 mm. The airfoil was pitched at the quarter chord, and the instantaneous angle of attack was written as $\alpha(t) = 0° \pm 6° \sin(\omega t)$. The variation of instantaneous angle of attack was confirmed by measurement with an encoder, and the measured instantaneous angle of attack was well matched with $\alpha(t) = 0° \pm 6° \sin(\omega t)$ [10].

Reverse flow and near wake were visualized by smoke-wire flow visualization. Fig. 1 shows the locations of the light source and the camera in the test section. A Teikoku alloy wire with a diameter of 0.14 mm was horizontally installed 3 mm downstream from the trailing edge. A sheet beam was generated by using six 1 kW halogen illuminators, and a Nikon F-100 camera with a shutter speed of 1/200 s was used. When implementing unsteady flow visualization, the operation time of the camera must be controlled to take pictures at the desired angle of attack. Thus, a special synchronization system was designed using two electronic relay systems and was quantitatively handled by a personal computer. Through synchronized control, photographs could be taken at the optimum quantity of smoke.

In this study, aerodynamic characteristics were obtained by integrating the unsteady pressure coefficients measured through a pneumatic tubing (0.6 m length and 1 mm internal diameter). Essentially, when unsteady pressure is measured through a pneumatic tubing, the magnitude and phase of the unsteady pressure measured at the end of the pneumatic tubing are different from the actual pressure. The difference is basically due to the viscous damping generated in the pneumatic tubing and the resonance by the reflected wave in the closed volume of the pressure transducer. However, by estimating the pressure transfer function of the pneumatic tubing and employing spectral analysis, the distorted unsteady pressure can be corrected. The detailed method of spectral analysis and estimation of transfer function are well depicted in Kim et al. [13].

A pressure transducer (Model 239, Setra) with the measurable pressure range of ±0.25 in H_2O (about ±63 Pa) was employed to measure the unsteady pressure, which can be utilized to measure the low pressure with high accuracy. A total of 120 samples of unsteady pressure were measured during a cycle, and the trigger signal was simultaneously recorded using a simultaneous sample